JOURNAL OF MATERIALS SCIENCE **38** (2003) 3545–3552

Properties of binary TiO_2-SiO_2 composite particles with various structures prepared by vapor phase hydrolysis

BYOUNG-SOO LEE, DONG-JUN KANG, SUN-GEON KIM
Department of Chemical Engineering, Chung Ang University, 221, Huksuk-Dong, Dongjak-Ku, Seoul 156-756, Korea
E-mail: sgkim@cau.ac.kr

Various TiO_2/SiO_2 composite nanoparticles were prepared by vapor phase hydrolysis of Titanium Tetraisopropoxide (TTIP) and Tetraethylorthosilicate (TEOS) in a tubular reactor heated by electrical furnace by changing the methods of reactant mixing, the molar ratio of the precursors and the set temperature of the furnace. These variables affected the average size and the bulk composition of the particles as well as their morphological and crystalline structures. The morphological structures of the particles were reconfirmed as T-S, S-T and T/S as in the previous study. Various correlations were obtained between the molar ratio of the precursors, and the size, the composition and the TiO_2 main peak intensity of the particles as a parameter of the mode of reactant mixing. In general, it was found that high content of silicon constituent showed translucent envelopes surrounding primary particles, which increased the dispersion diameter of the particles, reduced the thermal stability, retarded the anatase-to-rutile transformation and the initial photocatalytic degradation of phenol in an aqueous solution.

1. Introduction

Fine TiO_2 particles have been widely used as a white pigment in the paint, plastic and paper industries, etc., due to their high refractive indices [1]. Recently, nano-sized TiO_2 particles with the size of one order of magnitude lower than before have also been developed for the application of their semiconducting properties to photocatalysts and UV shields [2–4]. To enhance the characteristics of the particles, SiO_2 has been added to them as shell, core [5–7] or in a dispersed phase [8–10] since the component introduced plays a role of controlling the photocatalytic activities and the refractive indices, and raising the compatibilities of the particle surface when dispersed in liquid or solid matrices. Furthermore, the composite particles even showed the synergetic effect of the composites such as the generation of new catalytic active sites due to the interaction of TiO_2 with SiO_2 [2]. Understanding of the structural characteristics of TiO_2/SiO_2 composite particles is, therefore of great importance in a wide range of applied science.

Based on many fragmentary one-step formation processes of the composite particles proposed [5–10], we prepared the composite particles with various kinds of structures which also differed in their chemical composition and average size simply by changing the methods of precursor mixing in our previous study on the equimolar hydrolysis of the corresponding alkoxides at fixed molar ratio [11, 12]. Binary metal oxides are well-known in the catalyst field. This is resulted from the surface acidity induced by doping [4] and the formation of Ti—O—Si bonds [3]. Anderson *et al.* (1995) [13] reported that and the photoactivity of the silica-incorporated titana prepared by a sol-gel technique was 3 times higher than that of the Degussa P25 when the titania/silica ratio was 3 to 7. Fu *et al.* (1996) [4] reported that 16 wt% silica in titania was an optimum mixture concentration for high photoactivity.

In this study, we now varied the molar ratio of two precursors such as Titanium Tetraisopropoxide (TTIP) and Tetraethoxyorthosilicate (TEOS) in addition to the modes of precursor mixing and the set temperature of furnace. Based on the investigation of the properties of the composite particles prepared under various conditions such as their morphologies, size, structure, bulk and surface chemical composition, and crystallinities, we tried to correlate them with each other. We also studied the photocatalytic activities of the composite particles with the different properties.

2. Experimental

2.1. Particle preparation

Fig. 1 shows a schematic diagram of the particle generation system used in this study. The details of the experimental apparatus and procedures are shown elsewhere [12]. In brief, reagent-grade Titanium tetraisopropoxide (TTIP), $Ti(OC_3H_7)_4$, Tetraethylothosilicate (TEOS), $Si(OC_2H_5)_4$, and H_2O were sprayed in three parallel ultrasonic nebulizers and carried by nitrogen gas as a carrier. The droplets of each component from its nebulizer were vaporized in the first of the two

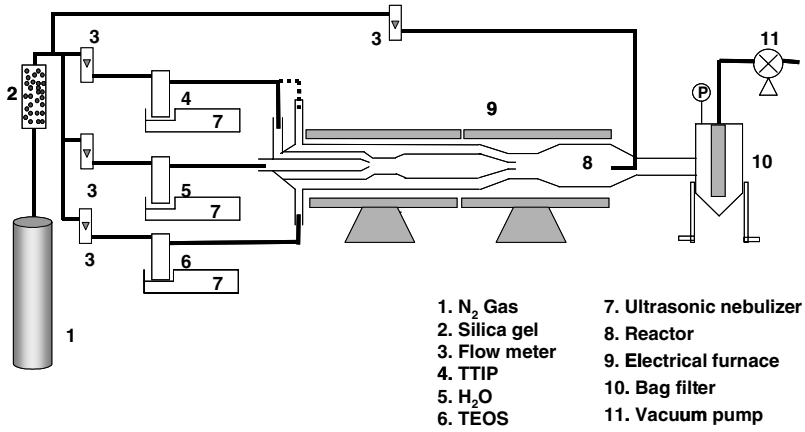

Figure 1 Experimental apparatus for composite particles.

consecutive temperature-controlled electrical furnaces until they meet and react each other in the second. With the spray rate of total alkoxides kept constant at about 18.4×10^{-6} mol/s, the molar ratio of TEOS to TTIP introduced into the reactor was varied from 0 to 1. The flow rate of the nitrogen gas through each nebulizer was 2l/min. The spray rate of H_2O was supplied at 5.4×10^{-3} mol/s which was highly excessive to react with the two alkoxides so as to maximize the relative chance of the hydrolysis with respect to the thermal decomposition and eliminate the effect of H_2O concentration on the hydrolyses and the successive particle formation. In order to prepare various forms of composite TiO_2-SiO_2 particles, TTIP, TEOS and H_2O were introduced and mixed in three different modes as indicated in Table I.

The temperatures set by the two furnaces were the same and varied from 350°C to 950°C with an interval of 200°C. In the temperature range we used, the hydrolysis reaction was always expected to play an important role but the thermal decomposition would not be excluded as the temperature increased, as indicated by Kirkbir *et al*. [14].

2.2. Characterization

The size and shape for the TiO_2-SiO_2 composite particles were observed with scanning electron microscope (SEM, JEOL Co., JSM-5200) and transmission electron microscope (TEM, Philips Co., CM-20). Size of the primary particles was obtained by measuring and averaging diameters of at least 100 particles in TEM images of each sample. Laser Particle Analyzer (LPA, Otsuka LPA-3100) was used to obtain the size distribution of the aggregates in colloidal solution after ultrasonic treatment in water for 5 min.

The crystalline structures of prepared TiO_2-SiO_2 composite particles were identified by powder X-ray diffraction analysis (XRD, SDS2000, Scintag). The bulk chemical composition was measured with Energy Disperse X-ray spectrophotometer attached to the TEM.

The chemical bonds in the particles were investigated with fourier-transform infrared spectroscopy (FT-IR, Perkin Elmer FT-IR 1615) and thermogravimeteric differential thermal analysis (TG-DTA, MAC Science, TG-DTA 200) was used to study the thermal stability of the particles.

TABLE I Reactant introduced to each inlet port in the following figure for the given method of mixing

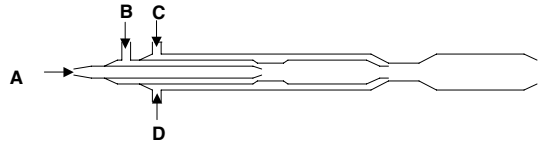

Configuration inlet port	T-S	S-T	T/S
A	H_2O	H_2O	H_2O
B	TTIP	TEOS	
C			TTIP
D	TEOS	TTIP	TEOS

2.3. Photocatalytic decomposition

The schematic of photocatalytic reactor are shown in Fig. 2. It is composed of a batch reactor with suspended catalyst particles, irradiation source and shielding. The reactor was made of quartz with a volume of 200 ml, whose temperature was controlled by a cooling coil immersed in the reactor. Initially, 0.05 g of the particles prepared under various conditions was suspended in the aqueous solution of phenol and methylene blue with the initial concentration of 100 ppm. During the

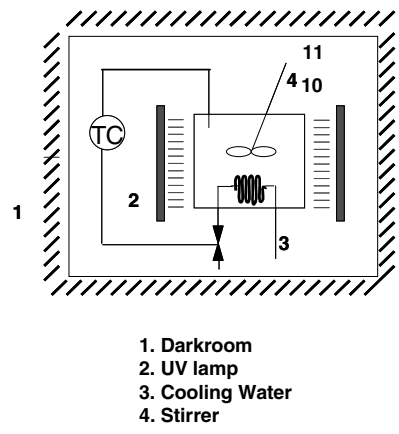

Figure 2 Experimental apparatus for photocatalytic reaction.

photocatalytic reaction, the reactor was well agitated to make the catalyst get UV evenly. As irradiation sources, four 10 W UV lamps were employed, each of which surrounded the reactor in square. The overall system was located in a dark box. During the UV irradiation, the concentration of the solute in the reactor was analyzed in every 30 min. Gas chromatography (HP 5890 Series 2) with a capillary column and flame ionization detector (FID) was used to quantify the unreacted phenol. The column temperature was 85°C and elevated to 115°C with the rate of 5°C/min. UV-VIS spectroscopy (UV-VIS, JASCO Model V-550) was also used to measure the absorbance of methylene blue.

3. Result and discussion

3.1. Morphologies

The various modes of TiO_2/SiO_2 composite particles, including TiO_2(core)-SiO_2(shell), SiO_2(core)-TiO_2(shell), TiO_2-SiO_2 mixed-type structures, were prepared according to the methods of reactant mixing. Fig. 3 shows TEM pictures, respectively, of the composite particles prepared with various mixing modes and initial precursor ratios. Core-shell structure is confirmed by the existence of a shell surrounding a core in single primary particles for the samples of S-T and T-S with the ratios of 0.2 and 0.5. On the other hand, the individual T/S particles show some mixed phase, even

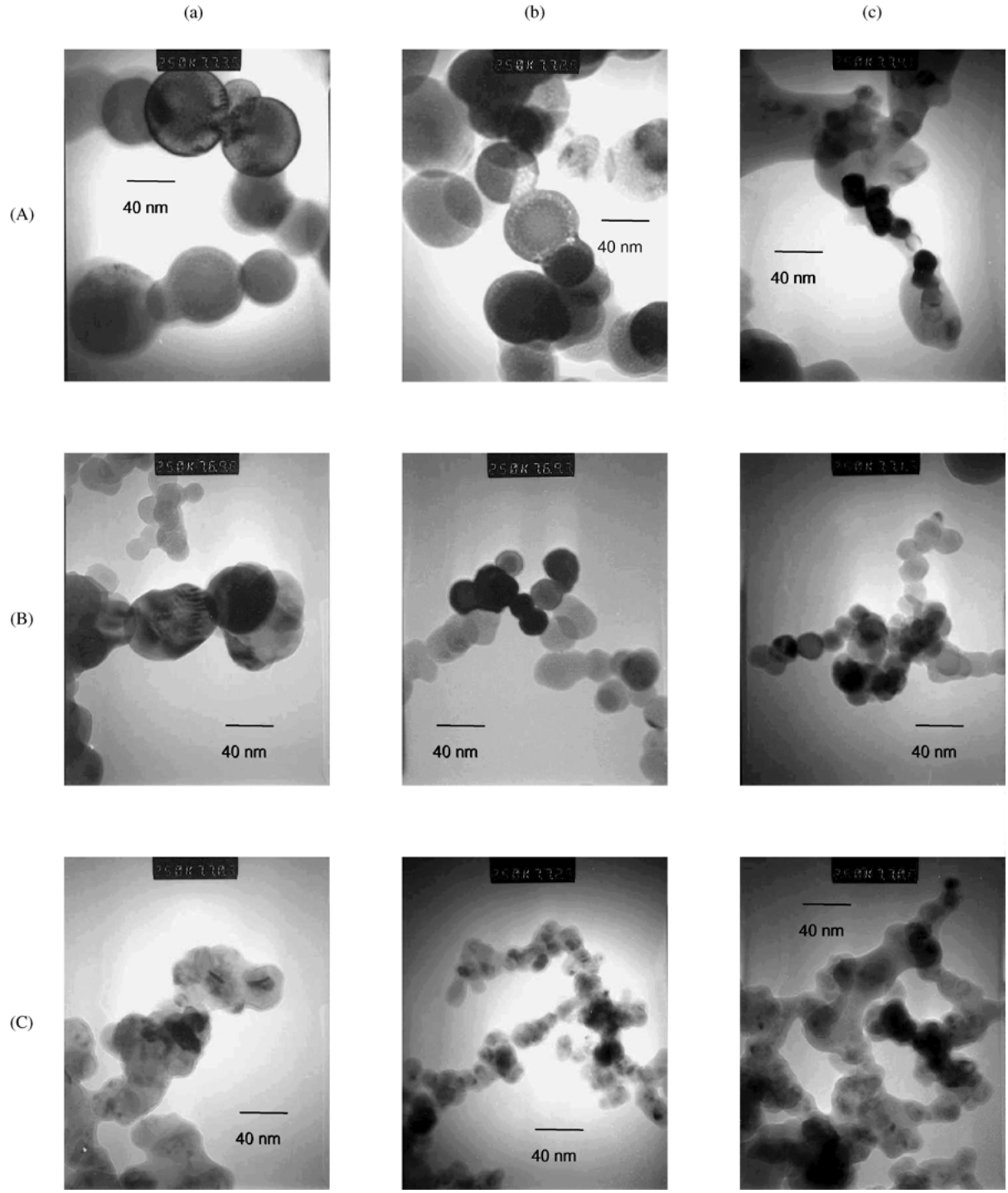

Figure 3 TEM images of various structures of composite particles prepared at 750°C (from left to right). (a) TTIP:TEOS = 0.8:0.2, (b) TTIP:TEOS = 0.5:0.5, and (c) TTIP:TEOS = 0.2:0.8 (from top to bottom). (A) S-T, (B) T-S, and (C) T/S.

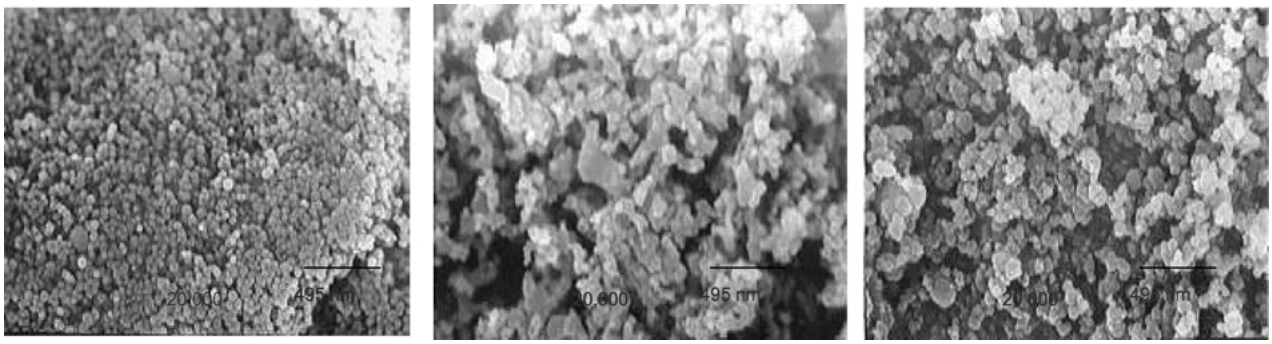

Figure 4 SEM images of (a) pure TiO_2, (b) S-T(TEOS:TTIP = 0.8:0.2) and (c) pure SiO_2 prepared at 750°C.

though individual particles are not in so well-mixed state of the two components as expected [12]. At the ratio of 0.8, the S-T particles and the T/S particles have translucent envelopes confining a lot of primary particles in them. They appear as not the aggregates having the identities of constituent primary particles but the irregularly shaped particles in SEM images as shown in Fig. 4b as well as the particles prepared from 100% TEOS as shown in Fig. 4c while pure TiO_2 particles appear as isolated primary particles as shown in Fig. 4a. The envelope of the silicon compounds in the S-T is anomalous since the shell of these particles would be TiO_2. This will be further discussed later. The average size of the primary particles decreases with the molar ratio of TEOS to TTIP shown in Fig. 5a as well as in order of S-T, T-S, T/S as shown in the previous study and. With the primary particle size decreasing, the degree of aggregation increases. In case of T/S particles with the smallest primary particle size of the three modes of mixing, the aggregation is most pronounced by the envelope of intermediate silicon compound even in the low TEOS/TTIP ratio.

3.2. Bulk chemical compositions

Fig. 5b shows the plot of silicon atomic ratio in the particles prepared with respect to the molar ratio of TEOS to TTIP. In case of T/S particles the silicon ratio increases approximately linearly with the initial reactant ratio with a concave curve upward. This means that the rate of TEOS conversion is not lower than that of TTIP in T/S mode of mixing at the temperature of 750°C. This supports the role of the surface area of small but many TiO_2 crystallites in the T/S mode [11, 12, 15]. The silicon fractions of T-S and S-T are lower than that of T/S and thus the curves for the T-S and the S-T are all convex upward. Therefore, without the help of TiO_2 surface exposed the rate of TEOS conversion is lower than that of TTIP [11, 12]. The fraction in T-S is close to that of T/S at a TEOS/TTIP ratio of 0.2 and thus higher than that of S-T while the order of silicon fractions of T-S and S-T is reversed at a ratio of 0.8. At the ratio of 0.5, the two modes result in almost the same silicon fraction. This implies that at lower ratio the availabilities of TiO_2 surface are similar in T/S and T-S and that of S-T is the lowest while at higher ratio TEOS unreacted to the cores later finds the surface of TiO_2 shell so that the additional envelope of silicon compounds can be formed as shown in the previous figure. As for the silicon content of the particles, the trend shown in the particle size is all reversed. Using Fig. 5a and b, the direct correlation of the particle size with silicon atomic ratio is obtained in Fig. 5c. The figure clearly shows retarding effect of silica on primary particle growth, and the precursor ratio and the mode of mixing ratio have more pronounced effect on the size of the primary particles than the silicon content.

3.3. Crystalline properties

Pure TiO_2 particles as prepared at the furnace set temperatures above 400°C showed anatase crystalline structure while pure SiO_2 particles were amorphous as prepared over the whole ranges of the temperatures. This implied that the decrease in height of XRD main peak would be a measure of the content of SiO_2, as shown previously by the corresponding author [12]. Fig. 6a shows the plots of the main peak height of the particles prepared with the different modes of mixing vs. the initial TEOS/TTIP molar ratio, and Fig. 6b shows the plots of the main peak height vs. the silicon atomic fraction in the particles where the initial TEOS/TTIP molar ratio is also labeled. As shown in figure, the inclusion of amorphous SiO_2 suppresses the growth of TiO_2 crystallites, irrespective of their structures. It is important that the crystalline peak decreased with the order of S-T, T-S, and T/S at fixed silicon atomic fraction. This supports that TiO_2 crystallites in the T/S structure exist in most isolated state. By the same token, since the mass of TiO_2 in T-S cores is lower than that in the shell of S-T and is confined in SiO_2 shells and their crystalline growth was thus more limited than that of the S-T particles. It is noted that the main peak height of the T-S particles is close to that of T/S particles at low TEOS/TTIP ratio while to that of the S-T particles at high ratio. This implies that the envelope of the silicon compounds for high TEOS/TTIP ratio also confines the TiO_2 shells of the S-T particles.

3.4. Chemical bonds

Fig. 7 shows the IR spectra of the composite particles prepared with various TEOS/TTIP molar ratios at 750°C. Inherent peaks of Ti─O and Si-O bonds are observed at 600–900 cm^{-1} and 1100 cm^{-1}, respectively, in all structures, which varied their depths with the

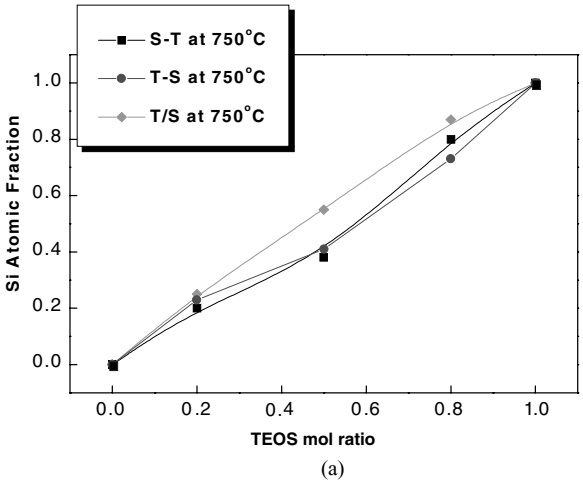

(a)

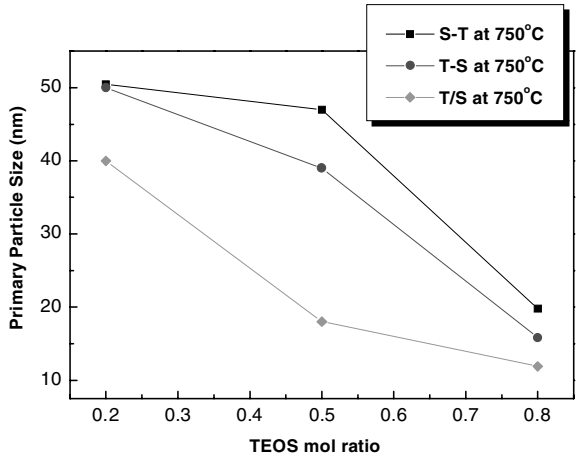

(b)

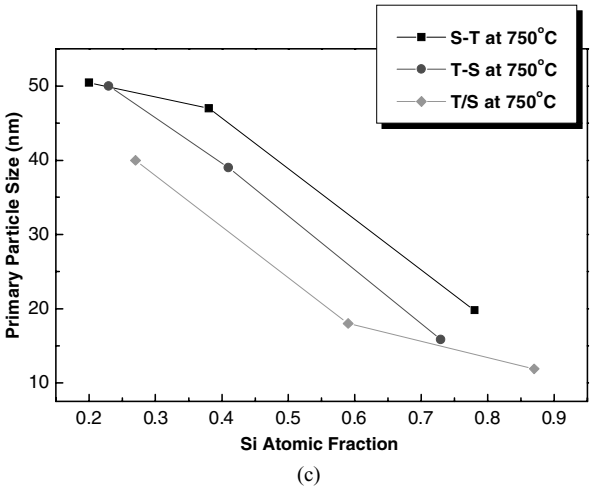

(c)

Figure 5 Correlations between: (a) silicon atomic fraction of primary particles and the initial TEOS/TTIP molar ratio, (b) the size of primary particles and the TEOS/TTIP molar ratio, and (c) the size and the silicon atomic fraction of primary particles.

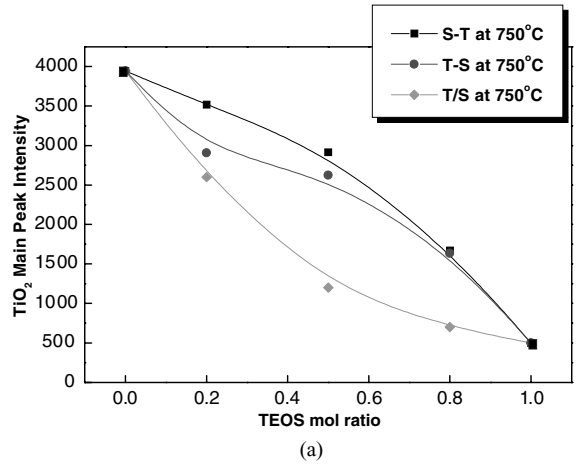

(a)

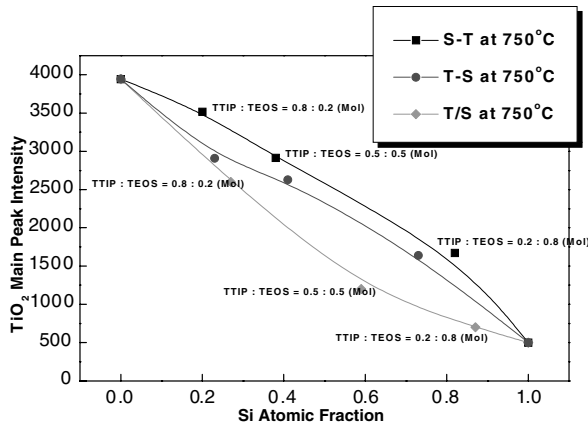

(b)

Figure 6 Correlations between: (a) TiO_2 main peak Intensity and the initial TEOS/TTIP ratio and (b) the TiO_2 main peak Intensity and the silicon atomic fraction.

contents of the corresponding components. While the peak of chemical Ti—O—Si bonding at 930 cm^{-1} is not observed at TEOS/TTIP ratio of 0.2, it appears at the ratios above 0.5, irrespective of the mixing modes, even though it is the weakest in the S-T particles. From the results, the intensity of chemical bonding of Ti—O—Si increases for the composite particles with high interfacial area between TiO_2 and SiO_2. The broad peaks of OH bond are observed at 3000–3500 cm^{-1} for all the samples, irrespective of the modes of mixing, with the initial TEOS/TTIP molar ratio of 0.8. They are prominent for the S-T and T/S, indicating the OH bonds are originated from the intermediates on the way to SiO_2.

3.5. Thermal stability

Fig. 8a is the results of TG-DTA for the particles prepared at 750°C with different modes of mixing. The weight losses ranging from 2 to 5% are related with the decomposition of intermediate products from precursor alkoxides [12]. The order of increasing weight loss is S-T, T-S and T/S, which is coincided with the order of increasing silicon atomic fraction. Due to the low hydrolysis rate of TEOS, the highest weight loss of the T/S particles was caused by the highest inclusion of silicon intermediates to oxide. This is also manifested by the fact that the weight loss is more pronounced for the sample prepared from higher TEOS/TTIP ratio, shown in Fig. 8b. Fig. 9 shows the DSC results for the particles prepared at 750°C with the different modes of mixing. There are two kinds of bumps for the particles of each mode. The first bumps appeared at 760°C for S-T and T-S particles and 900°C for T/S particles while the second bumps appeared around 1200°C for all the modes of particles. The first bumps indicate anatase-to-rutile transformation [16]. The order of the transformation

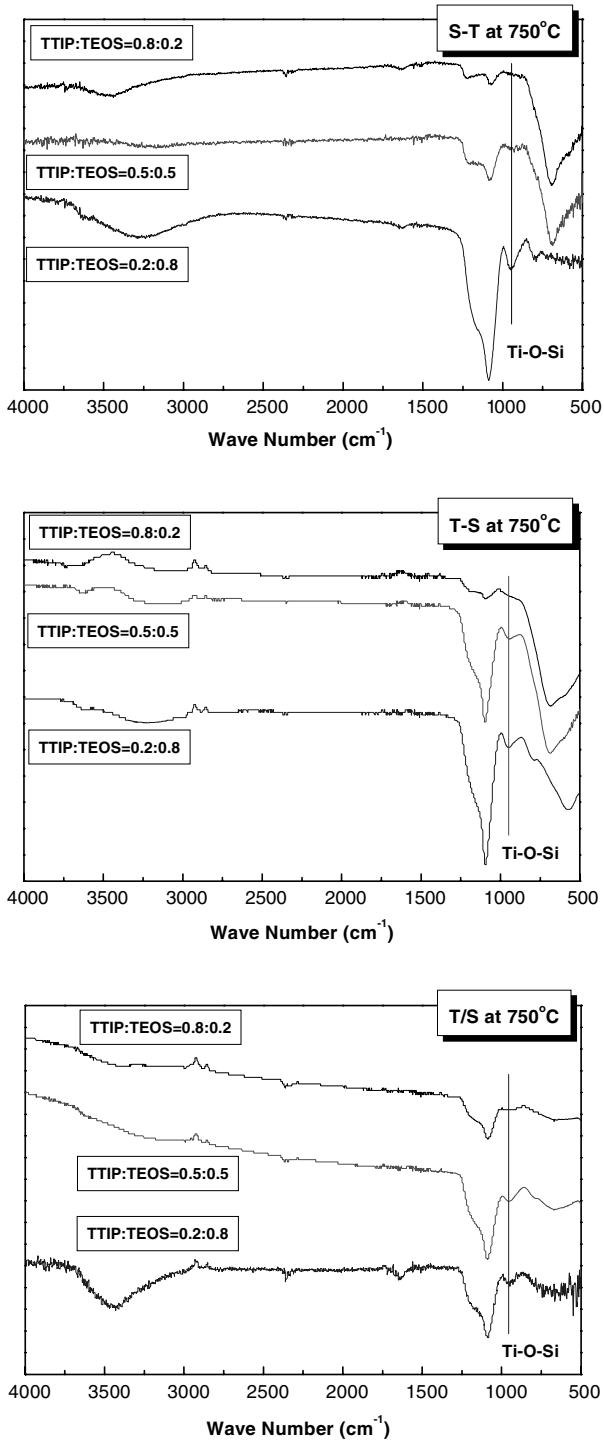

Figure 7 FT-IR spectra for particles prepared with the different modes of mixing and initial precursor ratio at 750°.

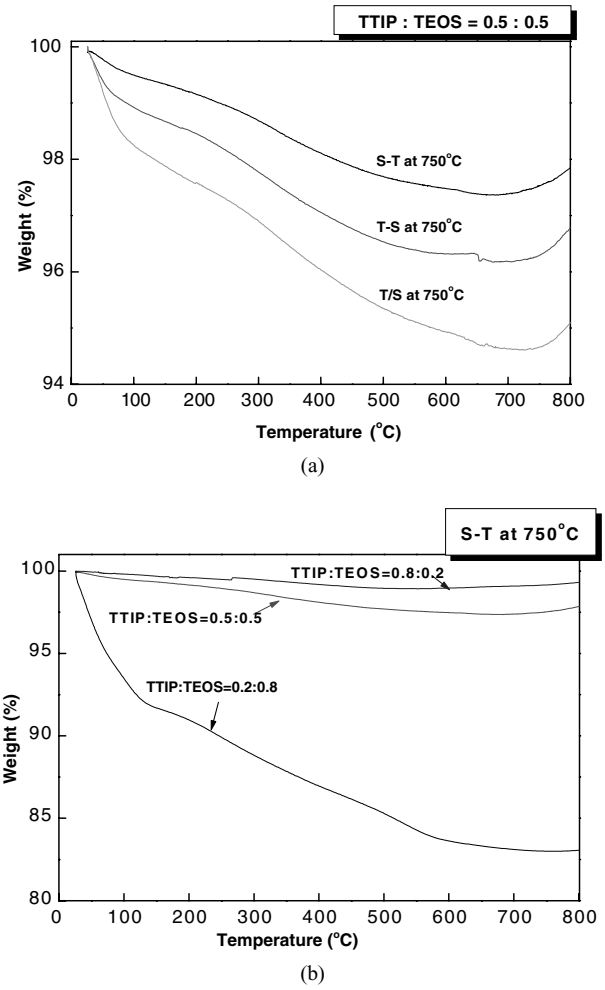

Figure 8 Thermogravimetric analysis of composite particles prepared: (a) with different modes of mixing and (b) with different initial TEOS/TTIP molar ratio.

temperature coincides with that discussed in the previous study [12]. The T/S particles have the highest difficulty in such transformation by the highest retardation effect of SiO_2 phase, due to TiO_2 relatively well dispersed in them.

3.6. Aggregation of composite particles

Fig. 10 shows average dispersive diameters of aggregates composed of composite particles in solution by Laser Particle Size Analyzer (LPA). It was shown in TEM images before that the average size of primary particles increased in order of T/S, T-S and T/S. However, as for LPA diameter, the trend is reversed. It means that the smaller the primary particles the larger their aggregates. It is nothing but the fact that aggregation occurs more easily between smaller particles. The LPA sizes increase substantially with the TEOS/TTIP ratio in each mode of precursor mixing. Under the conditions, translucent silicon intermediates enveloping the primary particles formed, which increased the size of aggregates. In general, it is concluded that the increase of silicon content in all structures drew aggregation among the particles.

3.7. Structural effect on photocatalytic activity

Fig. 11 shows the fractional conversion of phenol measured at 30 min, using the composite particles prepared at 750°C with the various modes of mixing and the fixed molar ratio of the precursors. The result for Degussa P-25 is also shown, whose fraction is close to that of the T/S, the lowest of the three modes. The conversions decreased in the order of S-T, T-S and T/S. The silicon atomic fractions of the samples were 0.38, 0.41, and 0.55, respectively, which are all larger than the optimal fractions of silicon. The latters ranged from 0.16 [4] to 0.30 [2]. Although it was pointed out that

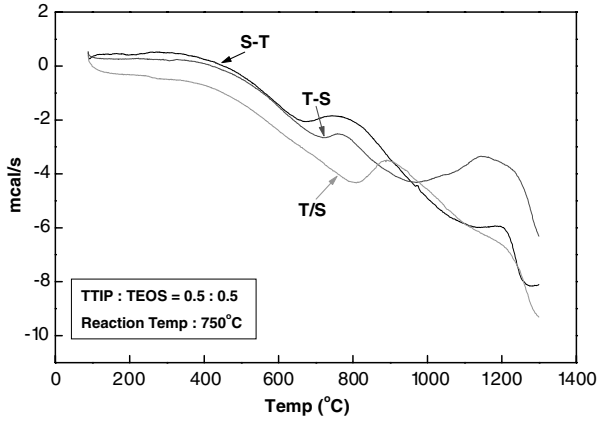

Figure 9 Differential scanning calorimetry of composite particles prepared with different modes of precursor mixing.

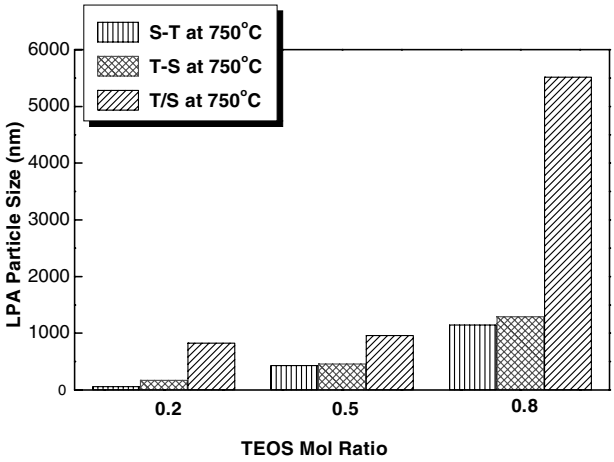

Figure 10 LPA diameters of various composite particles prepared at different TEOS/TTIP molar ratio.

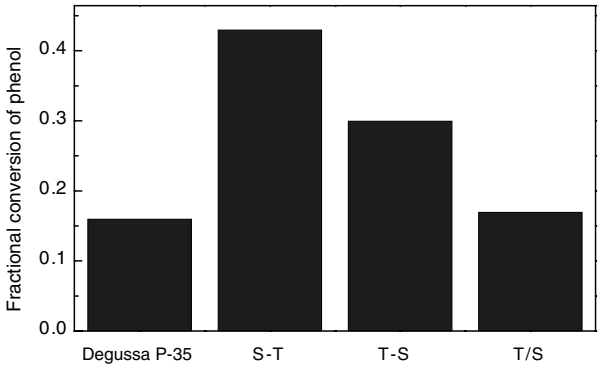

Figure 11 Fractional conversion of phenol in photocatalytic degradation by the composite particles prepared with different modes of mixing at 750°C. That for Degussa P-25 is also shown.

the structure of the photocatalysts has a lot of influence on the catalyst activity, nothing is known for the structures of the particles they used. Our samples were all in anatase, which was better form for the phtocatalysts. Fig. 12 shows the time evolution of the photocatalytic conversion of methylene blue by the composite particles prepared at 550°C. It is noted that for the particles prepared at 550°C and 750°C little structural difference was observed and the silicon fractions were 0.17, 0.18 and 0.27 for S-T, T-S and T/S, respectively [12]. Even

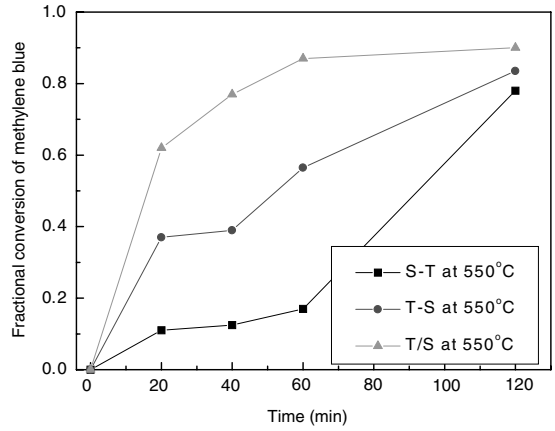

Figure 12 Time evolution of fractional conversion of methylene blue by the composite particles prepared with different modes of mixing at 750°C.

though the range of silicon content was within the optimal values shown in the literature [2, 4], the order of the initial conversion is still the same as that of phenol by the particles prepared at 750°C. This order of decreasing conversion coincided with that of the thickness of the SiO_2 surrounding TiO_2 crystallites, or the degree of TiO_2 hiding in the particle matrices. Fig. 12 also shows that the ultimate conversions, irrespective of the modes of precursor mixing. These imply that the photocatalytic reaction depends on the exposed area of TiO_2, and the higher the degree of TiO_2 hiding, the lower the rate of the reaction since the diffusion of chemical species needs time to pass through the inert SiO_2 film. We are still finding an optimal condition for photocatalytic activity of the composite particles.

4. Conclusion

Vapor-phase preparation of TiO_2-SiO_2 mixed, TiO_2(core)-SiO_2(shell) and SiO_2(core)-TiO_2(shell) have been reproduced by the same method in the previous study. The initial molar ratio of the corresponding alkoxides was varied in full range in this study. The major previous findings of the study were confirmed by more reasonable evidences such as the visual structures of the particles, the role of the translucent silicon intermediates, the correlations between the size, the chemical composition and the crystallinity of the particles, the thermal stability and the photocatalytic activity of the particles. The lower rate of TEOS resulted in incomplete conversion to SiO_2 and thus the translucent envelopes were formed from the reaction with high TEOS/TTIP ratio. The silicon content increased the dispersion diameters in the aqueous suspension, lowered the particulate thermal stability, and retarded the primary particle growth, the anatase-to-rutile transformation during the subsequent heat treatment and the initial photocatalytic reaction.

Acknowledgement

This research is supported by the Chung Ang University Research Grants in 2001.

References

1. Y. L. LIN, T. J. WANG and Y. JIN, *Powder Technol.* **123** (2002) 194.
2. C. ANDERSON and A. J. BARD, *J. Phys. Chem.* **99** (1995) 9882.
3. X. GAO and I. E. WACHS, *Catalysis Today* **51** (1999) 233.
4. X. FU, L. A. CLARK, Q. YANG and M. A. ANDERSON, *Environ. Sci. Technol.* **647** (1996) 30.
5. Q. H. POWELL, G. P. FOTOU, T. T. KODAS and B. ANDERSON, *J. Aerosol Sci.* **26** (1995) S557.
6. S. JAIN, T. T. KODAS, M. K. WU and P. PRESTON, *ibid.* **28** (1997) 133.
7. S. H. EHRMAN, S. K. FRIEDLANDER and M. R. ZACHARIAH, *ibid.* **29** (1998) 687.
8. Y. SUYAMA, E. URA and A. KATO, *Jap. J. Chem. Soc. (Japan)* (1978) 356.
9. M. K. AKHTAR, S. PRATSINIS and S. V. R. MASTRANGELO, *J. Amer. Ceram. Soc.* **75**(1992) 3408.
10. G. P. FOTOU, T. T. KODAS and B. ANDERSON, *Aerosol Sci. Technol.* **33** (2000) 557.
11. S. K. LEE, K. W. CHUNG and S. G. KIM, *ibid.* **36** (2002) 763.
12. W. H. CHO, D. J. KANGCHUNG and S. G. KIM, *AJ. Mater. Sc.* Submitted (2002).
13. C. ANDERSON and A. J. BARD, *J. Phys. Chem.* **9882** (1995) 99.
14. F. KIRKBIR and H. KOMIYAMA, *Chem. Lett.* (1988) 791.
15. Y. SUYAMA, E. URA and A. KATO, *Jap. J. Chem. Soc. (Japan)* (1978) 356.
16. E. MATIJEVIC, Q. ZHONG and R. E. PARTCH, *Aerosol Sci. Technol.* **22** (1995) 162.

Received 27 January
and accepted 20 May 2003